Proceedings of the 20th National Conference on Superconductivity "New Phases, Concepts and Advances"

Berezinskii–Kosterlitz–Thouless Transition in Ultrathin Niobium Films

S.M. Altanany*, I. Zajcewa, R. Minikayev and M.Z. Cieplak

Institute of Physics, Polish Academy of Sciences, al. Lotników 32/46, PL-02668 Warszawa, Poland

Doi: 10.12693/APhysPolA.143.129 *e-mail: altanany@ifpan.edu.pl

We use resistivity and current–voltage characteristics measurements to evaluate the impact of the disorder on the nature of the Berezinskii–Kosterlitz–Thouless transition in ultrathin niobium (Nb) films. The films, with thickness in the range of 3.6–8.5 nm, show the structural transition from polycrystalline to amorphous structure upon a decrease in the film thickness. We show that this transformation results in the smearing of the Berezinskii–Kosterlitz–Thouless transition, until eventually the Berezinskii–Kosterlitz–Thouless scenario breaks down due to film inhomogeneity.

topics: superconducting films, niobium films, inhomogeneity

1. Introduction

The characteristic feature of 2-dimensional (2D) homogeneous superconductors (SC) is the occurrence of Berezinskii–Kosterlitz–Thouless (BKT) transition at the temperature T_{BKT}, below mean-field transition temperature T_{c0}, $T_{\mathrm{BKT}} < T_{c0}$. The BKT transition, first predicted theoretically on the basis of the 2D XY model [1, 2] and subsequently observed experimentally in many SC films [3–5], is associated with the thermal unbinding of vortex–antivortex pairs, which gives rise to finite resistance in the temperature range $T_{\mathrm{BKT}} < T < T_{c0}$. A distinct signature of the BKT transition is present in the current–voltage (I–V) characteristics, which evolve from nonlinear to linear upon approaching the normal state with increasing temperature.

A BKT transition is commonly studied through two distinct approaches. When approaching the transition from below, the superfluid stiffness J_s is expected to jump discontinuously from a finite value below T_{BKT} to zero, following the universal relation $J_s(T_{\mathrm{BKT}})/T_{BKT} = 2/\pi$. Here J_s is related to superfluid density n_s by the following relation $J_s = \hbar^2 n_s/4m^* = \hbar^2 c^2 d/(16\pi e^2 \lambda^2)$, where d is the film thickness and λ is the penetration depth. This condition may be verified by direct measurements of the penetration depth or by evaluation of the nonlinear exponent of the I–V characteristics. The second approach is that from above T_{BKT}. In this case, the T-dependence of various quantities, such as resistivity or magnetization, are affected by both the approach to BKT, and by the presence of Ginzburg–Landau (GL) fluctuations. The theory by Halperin and Nelson [6] suggests an interpolation formula, which includes both effects.

These two approaches have led to the successful identification of the BKT transition in many systems, including niobium (Nb) compounds [7, 8]. However, when the films are very thin, such as those studied in the present work, the structural disorder is expected to induce inhomogeneity in the SC state. This, in turn, may smear the BKT transition, complicating the interpretation of the results. The role of inhomogeneity in the smearing of the BKT transition has been addressed in recent years in the case of several systems [9, 10]. Nevertheless, to the best of our knowledge, the present work is the first study of the BKT transition in ultrathin Nb films. Moreover, we use films, in which we have previously uncovered structural transition from polycrystalline to amorphous structure upon a decrease in film thickness [11]. This allows for a direct evaluation of the influence of the disorder on the BKT transition. In the following, in order to unambiguously identify T_{BKT}, we utilize both approaches mentioned above.

2. Experimental details

Ultrathin Nb films of thickness d ranging from 3.6 to 8.5 nm have been deposited by a magnetron sputtering at room temperature on glass substrates. Nb layers are sandwiched between two silicon (Si) wafers for protection against oxidation. The thickness of the Nb layers has been determined by low-angle X-ray reflectivity measurements. More details about structural evaluation have been provided in previous publications [11, 12]. Briefly, the structure of Nb begins to transform from polycrystalline to amorphous when d falls below 5 nm, and it becomes completely amorphous when $d \approx 3.3$ nm. While the thick films ($d = 9.5$ nm) show a sharp

interface between Nb and Si, in the case of the thinnest films ($d = 1.3$ nm), a mixed interface layer rich in Nb is formed, $Nb_{1-x}Si_x$, with x of the order of 0.05–0.1.

The films are photolithographically patterned and etched with ion beam into Hall bar structures with a current-bar width of 200 μm and length of 2 mm. Electrical contacts are made across the current and voltage channels at the film surface with the aid of indium solder. Transport measurements have been done in the absence of a magnetic field ($B = 0$ T) by a standard four-probe measurement method using a Quantum Design physical property measurement system (PPMS).

3. Results and discussion

Figure 1 shows the temperature dependence of sheet resistance R_{sq} for three films of different thicknesses. A standard method used to determine T_{BKT} is to fit experimental resistance data to the interpolation formula proposed by Halperin and Nelson (H–N) [6, 13]

$$R_{sq}(T) \approx R_N \,\mathrm{const}\, \exp\left(-2\sqrt{\frac{b\,(T_{c0}-T_{\mathrm{BKT}})}{T-T_{\mathrm{BKT}}}}\right). \tag{1}$$

Here, T_{c0}, T_{BKT}, and dimensionless constants const and b are adjustable (sample-dependent) fitting parameters, and R_N is the normal-state sheet resistance determined from experimental data. The values of T_{BKT} and T_{c0} resulting from the fits, with R_N defined at $T = 10$ K, are shown in Fig. 1. In light of the BKT theory, the interval $(T_{c0} - T_{\mathrm{BKT}})$ is governed by the proliferation of vortex–antivortex pairs, which are thermally dissociated in the vicinity of T_{BKT}. This difference between the transition temperatures becomes more prominent for disordered films thanks to the broadening feature of the normal-to-superconducting phase transition associated with a modified crossover from BKT to the GL superconducting fluctuations.

There is another common way for the T_{BKT} extraction, which relays on the fact that in the vicinity of T_{BKT}, i.e., for $T<T_{c0}$, (1) may be approximated by the relation $R_{sq}(T)\approx R_0 \exp\left(-b_1(T-T_{\mathrm{BKT}})^{-1/2}\right)$ [14]. This leads to the following dependence

$$\left[\frac{\mathrm{d}\ln(R_{sq}(T))}{\mathrm{d}T}\right]^{-\frac{2}{3}} = \left(\frac{2}{b_1}\right)^{\frac{2}{3}}(T - T_{\mathrm{BKT}}). \tag{2}$$

A fit to the linear in T dependence of $[\mathrm{d}\ln(R_{sq}(T))/\mathrm{d}T]^{-\frac{2}{3}}$, shown in Fig. 2, results in T_{BKT} values nearly identical to those found using (1). However, an interesting and remarkable feature seen in Fig. 2 is the appearance of the finite value of the quantity $[\mathrm{d}\ln(R_{sq}(T))/\mathrm{d}T]^{-2/3}$ below T_{BKT} in films with $d < 5$ nm. Mathematically, it results from a tiny but finite value of R_{sq} at low temperatures, which is not expected in the case of true BKT transition. The finite value of R_{sq} may suggest that the SC state in these thinner films becomes increasingly inhomogeneous, so that the current used for these measurements, however small, destroys superconductivity locally. Since our data extend down to 2 K, we cannot exclude the possibility that R_{sq} will eventually drop to zero at lower T.

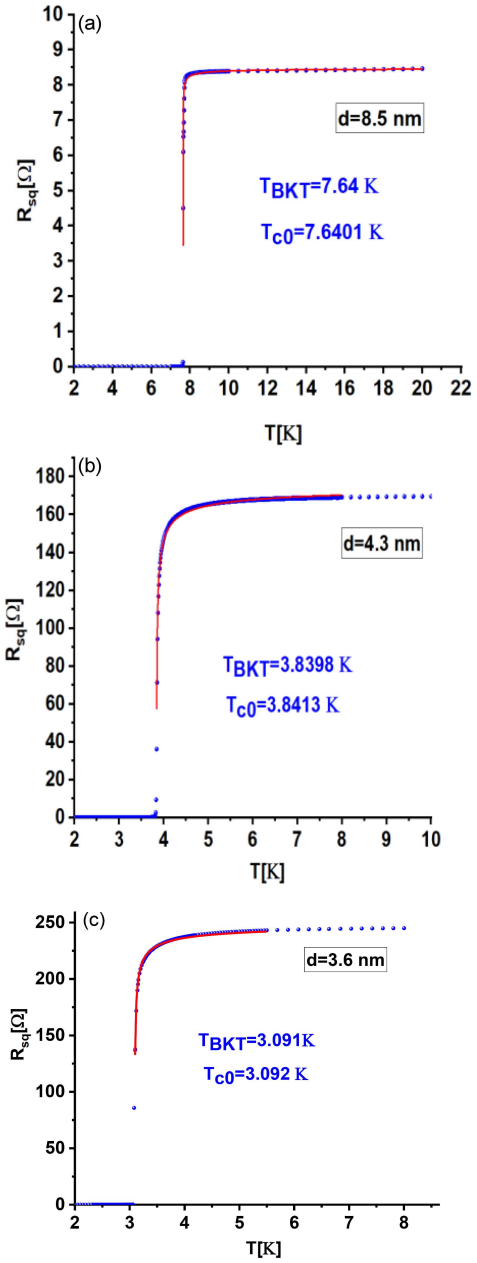

Fig. 1. Temperature dependence of sheet resistance, $R_{sq}(T)$, for Nb films with different d. Measurements were performed at different excitation currents ($I = 0.5$, 0.05, 0.1 mA, for $d = 8.5$, 4.3, 3.6 nm, respectively). The (red) solid lines correspond to theoretical fits of (1) to the data indicated by (blue) points. The values of T_{BKT} and T_{c0} are given in the figures.

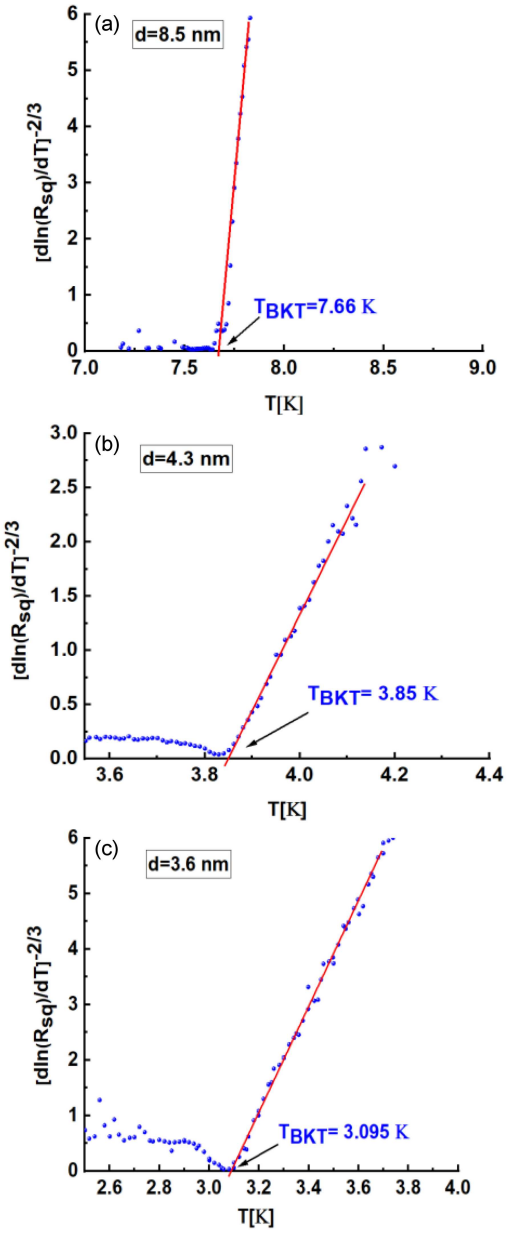

Fig. 2. Dependence $[\mathrm{d}\ln(R_{sq}(T))/\mathrm{d}T]^{-\frac{2}{3}}$ vs T for Nb films with $d = 8.5$, 4.3, 3.6 nm. Here, T_{BKT} (marked in the figures) are derived by extrapolation of the linear section as indicated by continuous (red) lines.

The evolution of the behavior of the I–V characteristics with decreasing film thickness is presented on a log–log scale in Fig. 3. It is observed that at high T the dependences may be described by the relation $V \propto I^{n(T)}$, with $n = 1$, independent of the value of the current, as expected for a normal state. In the case of the thickest of the three films (Fig. 3a), we mark by a dotted rectangle the region in which $\ln(V)$ is proportional to $\ln(I)$. In this region, $I(V)$ follows the power-law for all temperatures, with n increasing with decreasing T. This is typical behavior expected for a homogeneous SC state. Within the BKT scenario, it is expected that n increases rather abruptly from 1 in the normal state to 3 at $T = T_{\mathrm{BKT}}$, following the jump of J_s from 0 to $2/\pi$ as T is reduced below T_{BKT} [15]

$$n(T) = 1 + \frac{\pi J_s(T)}{T}. \tag{3}$$

At even lower $T < T_{\mathrm{BKT}}$, vanishing dissipation is expected in the limit of low currents for all temperatures, implying a divergence of n on the approach to $T = 0$. And indeed, this is what can be seen in Fig. 3a, so we can confidently estimate that T_{BKT} is within the range of 7.62–7.63 K at $n = 3$, as shown by the dashed red line inside the dotted rectangle. This value is somewhat smaller but still quite close to the values extracted from relations (1) and (2).

Note that in the region of the plot above the rectangle, i.e., at high V at each given T, the values of V show saturation before jumping abruptly to a high value in the normal state. The saturation most likely indicates the occurrence of flux flow, which precedes an abrupt jump to a normal state. As temperature is increased, the jump broadens, which may lead to an artificial "$n = 3$" slope appearing in the high-V region of the plot (dashed green line). We believe that this high-V, high-I region is not an appropriate range to define T_{BKT}, as it is sometimes done in literature, because it is, in fact, an incipient jump into a normal state. If we try to use it and plot in this high-V range a dashed green line with slope $n = 3$, we get values of T_{BKT} in the range of 7.64–7.65 K, slightly higher than obtained from the low-V range. Nevertheless, we see that in the case of a homogeneous film with $d = 8.5$ nm, the error in the value of T_{BKT} extracted from the high-V range is not large.

The situation is different in thinner films. In Fig. 3b, we show that the evolution of the I–V characteristics is somewhat similar to that of the thickest film, i.e., with the decrease in T, we observe the increase in the slope of the $V(I)$ on a log–log plot in the region of small V. However, we also observe that the region of power-law dependence (inside dotted rectangle) is restricted to smaller I and V, particularly at low T. Still, we can identify isotherms in the vicinity of $n = 3$. We find that T_{BKT} extracted from the low-V region is significantly lower than that extracted from the high-V region (both values are shown in the figure caption), and it is also lower than that obtained from resistivity analysis. An even more profound discrepancy exists in the case of the thinnest film (Fig. 3c), for which I–V in the low-V range indicates the absence of the BKT transition down to 2 K. On the other hand, both the high-V range (green dashed line) and resistivity analysis suggest finite T_{BKT}. The possible explanation for this large discrepancy is the film inhomogeneity, which leads to an inhomogeneous SC state, possibly in the form of SC puddles with different strengths of SC condensate or SC puddles immersed in the non-SC matrix. This results in the

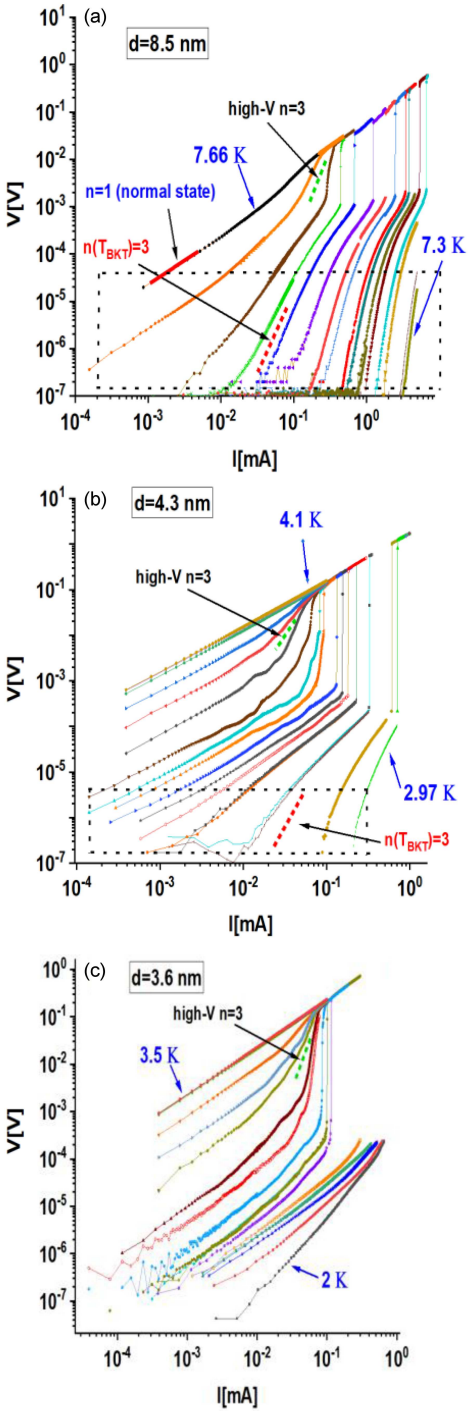

Fig. 3. Behavior of I–V isotherms on a log–log scale at different temperatures for films with d = 8.5 nm (a), $d = 4.3$ nm (b), and $d = 3.6$ nm (c). The dashed rectangle in (a) shows low $V(I)$ regime with power-law behavior. Red (green) dashed lines are drawn at $n = 3$ in the low-V (high-V) regions. From (a) $T_{\rm BKT}$ is between 7.62–7.63 K for $d = 8.5$ nm, and from (b) it is between 3.31–3.58 K for $d = 4.3$ nm. No BKT transition is observed down to 2 K in the low-V regime for $d = 3.6$ nm (c). In the high-V regions, the $n = 3$ isotherm is located between 7.64 K and 7.65 K for $d = 8.5$ nm, between 3.83 K and 3.84 K for $d = 4.3$ nm and between 3.09 K and 3.11 K for $d = 3.6$ nm.

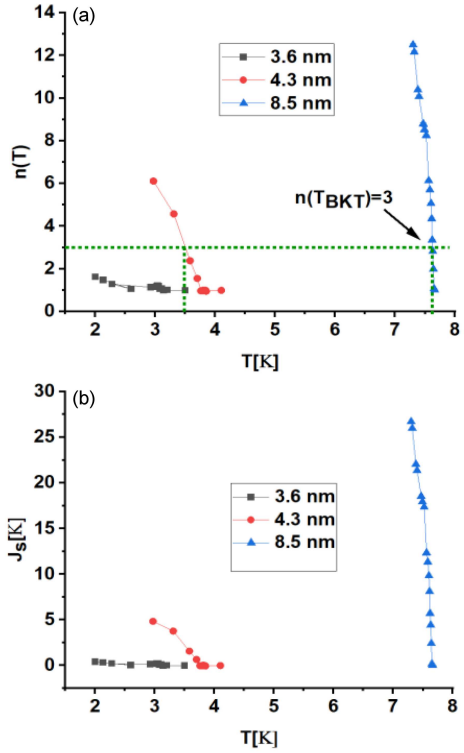

Fig. 4. Dependence $n(T)$ (a), and $J_s(T)$ (b) for films with different thickness. From (a) we estimate $T_{\rm BKT} = 3.49$ K for $d = 4.3$ nm.

distribution of $T_{\rm BKT}$ values across the film, and I–V measurements capture this in the form of a gradual change of the slope n in the vicinity of $T_{\rm BKT}$. On the other hand, in the course of resistivity analysis, we assume the single value of $T_{\rm BKT}$ and make the fits of (1) or (2) at $T > T_{\rm BKT}$. This results in the overestimation of $T_{\rm BKT}$ in the case of an inhomogeneous system, as discussed extensively in [16]. We also note that the inhomogeneity broadens the incipient jump into the normal state in the high-V region, so it can be easily mistaken for a curve with $n = 3$ slope. We conclude that it is the I–V characteristics in the low-V range that reveals the true behavior of the BKT transition.

Finally, in Fig. 4, we show the T-dependences of the exponent n and of J_s, estimated using (3). As anticipated, the universal jump in $J_s(T)$ from normal to SC state is smeared upon decreasing thickness. In the case of the thinnest film, J_s is very small, and no BKT transition may be identified down to 2 K.

We note here that the effect of disorder on the smearing of J_s jump has been discussed in many experimental and theoretical studies [10, 17, 18]. Systems with various forms of inhomogeneity have been studied, including the most common assumption that the disorder in thin films leads to fragmentation of the SC state due to localization effects, or that the fragmentation of the SC state is induced by extrinsic factors due to various properties

of the film substrates. Regarding the present case, we have shown in the previous study [11] that the Nb films undergo a structural transformation, from the amorphous structure for $d < 3$ nm, to a mixed amorphous/polycrystalline structure for $3 < d < 5$ nm, and to a fully polycrystalline structure for $d > 5$ nm. This strongly suggests that the primary reason for the behavior of the BKT transition in the present case is the film inhomogeneity triggered by this structural transformation.

4. Conclusions

We have studied the evolution of BKT transition in ultrathin Nb films with decreasing film thickness, using analysis of the resistivity and the I–V characteristics. While in the thicker, polycrystalline film, we consistently identify the BKT transition using these different methods, we observe discrepancy in the results when the structure of the films changes into amorphous, suggesting that the film inhomogeneity triggered by structural transformation contributes primarily to the behavior of the BKT transition.

Acknowledgments

We are grateful to Leyi Y. Zhu and C.L. Chien (Johns Hopkins University) for growing the films used in this study.

References

[1] J.M. Kosterlitz, D.J. Thouless, *J. Phys. C Solid State Phys.* **6**, 1181 (1973).

[2] J.M. Kosterlitz, *J. Phys. C Solid State Phys.* **7**, 1046 (1974).

[3] Y. Xing, J. Wang, *Chinese Phys. B* **24**, 117404 (2015).

[4] H. Toyama, R. Akiyama, S. Ichinokura et al., *ACS Nano* **16**, 3582 (2022).

[5] T. Ren, M. Li, X. Sun, L. Ju, Y. Liu, S. Hong, Y. Sun, Q. Tao, Y. Zhou, Z.-A. Xu, Y. Xie, *Sci. Adv.* **8** 1 (2022).

[6] R.J. Londergan, J.S. Langer, *Phys. Rev. B* **5**, 4376 (1972).

[7] M.V. Burdastyh, S.V. Postolova, T. Proslier, S.S. Ustavshikov, A.V. Antonov, V.M. Vinokur, A.Yu. Mironov, *Sci. Rep.* **10**, 1471 (2020).

[8] E. Khestanova, J. Birkbeck, M. Zhu et al., *Nano Lett.* **18**, 2623 (2018).

[9] M. Mondal, S. Kumar, M. Chand, A. Kamlapure, G. Saraswat, V.C. Bagwe, J. Jesudasan, L. Benfatto, P. Raychaudhuri, *J. Phys. Conf. Ser.* **400**, 022078 (2012).

[10] G. Venditti, J. Biscaras, S. Hurand et al., *Phys. Rev. B* **100**, (2019).

[11] I. Zaytseva, O. Abal'oshev, P. Dłużewski, W. Paszkowicz, L.Y. Zhu, C.L. Chien, M. Kończykowski, M.Z. Cieplak, *Phys. Rev. B* **90**, 060505(R) (2014).

[12] I.N. Demchenko, W. Lisowski Y. Syryanyy, Y. Melikhov, I. Zaytseva, P. Konstantynov, M. Chernyshova, M.Z. Cieplak, *Appl. Surf. Sci.* **399**, 32 (2017).

[13] A.F. Hebard A.T. Fiory, *Phys. Rev. Lett.* **44**, 291 (1980).

[14] J.H. She, A.V. Balatsky, *Phys. Rev. Lett.* **109**, 1 (2012).

[15] D.R. Nelson, J.M. Kosterlitz, *Phys. Rev. Lett.* **39**, 1201 (1977).

[16] L. Benfatto, C. Castellani, T. Giamarchi, *Phys. Rev. B* **80**, 1 (2009).

[17] R.W. Crane, N.P. Armitage, A. Johansson, G. Sambandamurthy, D. Shahar, G. Grüner, *Phys. Rev. B* **75**, 1 (2007).

[18] I. Maccari, L. Benfatto, C. Castellani, *Condens. Matter* **3**, 8 (2018).